JOURNAL OF MATERIALS SCIENCE **35** (2000) 4487 – 4493

Thermal conductivity of unidirectionally oriented Si_3N_{4w}/Si_3N_4 composites

S. W. LEE
Sun Moon University, Department of Materials Engineering, Asan, 336-840, South Korea
E-mail: swlee@omega.sunmoon.ac.kr

H. B. CHAE
Sunchunhyang University, Department of Physics, Asan, 336-840, South Korea

D. S. PARK
Korea Institute of Machinery and Materials, Changwon, 641-010, South Korea

Y. H. CHOA, K. NIIHARA
ISIR, Osaka University, Osaka, 567-0047, Japan

B. J. HOCKEY
National Institute of Standards and Technology, Gaithersburg, MD, 20899, U.S.A.

β-silicon nitride whiskers were aligned unidirectionally in silicon nitride sintered with 2 wt% Al_2O_3 and 6 wt% Y_2O_3. It was be densified by the Gas Pressure Sintering (GPS) method. Thermal conductivity of the sintered body with different amount of β- silicon nitride whiskers was measured by the direct contact method from 298 K to 373 K. This unidirectionally oriented β-silicon nitride whiskers grew into the large elongated grains, and improved also the thermal conductivity. The amount of β-silicon nitride whiskers changed the microstrcuture, which changed the thermal conductivity. © *2000 Kluwer Academic Publishers*

1. Introduction

Silicon nitride is one of the leading materials available for gas turbines and other high temperature structural applications because of its superior oxidation, thermal shock resistance, and mechanical strength (high toughness, high strength, excellent creep resistance). Si_3N_4 is commonly obtained by the addition of a metal oxide (e.g. MgO, Al_2O_3, and Y_2O_3) as a sintering aid. However, its mechanical properties degrade at the high temperatures above 1473 K because of glassy grain boundaries. As for Si_3N_4 ceramics with MgO or Y_2O_3, the grains were a well-developed hexagonal shape. From a practical standpoint, the thermal properties (thermal expansion coefficient, thermal diffusivity, specific heat and thermal conductivity) of silicon nitride are of extreme importance for the high temperature applications. The thermal properties of hot pressed Si_3N_4 (HP-Si_3N_4), hot isostatic pressed Si_3N_4 (HIP-Si_3N_4), and reaction bonding sintered Si_3N_4 (RS-Si_3N_4) have been investigated by many workers [1–8]. Chemical vapor deposited Si_3N_4 (CVD-Si_3N_4) which had crystalline phase, amorphous phase, or a mixture of both. Hirai *et al.* [1] measured thermal diffusivity and thermal conductivity by a laser flash method in the range of 293 to 1574 K. The structure of CVD-Si_3N_4 was crystalline or amorphous, depending on the deposition temperature and total pressure. At 293 K, the thermal diffusivity for crystalline CVD-Si_3N_4 was about 25 times greater than that for amorphous CVD-Si_3N_4. The thermal diffusivity of RS-Si_3N_4 was considerably higher because of a continuous metal phase of free silicon.

The experiments to increase thermal conductivity of silicon nitride by modifying the powder and sintering processing have been carrying out since Haggerty *et al.* [9] reported that the theoretical value of thermal conductivity in the intrinsic silicon nitride is 200 Wm^{-1} K^{-1}. Recently it has been reported that the addition of the rare earth oxide as the sintering additives increased the thermal conductivity of silicon nitride. The thermal conductivity as high as 120 Wm^{-1} K^{-1} can be obtained if the long heat treatment at high temperatures (2273 K, 3 MPa in N_2 gas, 4 hours) are employed [10]. Similarly to this processing, the addition of β-silicon nitride whisker improved thermal conductivity of silicon nitride [11].

In this study, β- silicon nitride whiskers were aligned unidirectionally in silicon nitride sintered with 2 wt% Al_2O_3 and 6 wt Y_2O_3. It was be densified by the Gas Pressure Sintering (GPS) method. Thermal conductivity of the sintered body with different amount of β -silicon nitride whiskers was measured by the direct contact method from 298 K to 373 K. The amount of β-silicon nitride whiskers may change the microstrcuture, which changes the thermal conductivity.

2. Experimental procedure

2.1. Sample preparation

The UBE E-10 silicon nitride powder (α-Si_3N_4, average particle size of 200 nm, UBE Industries, Tokyo, Japan) with 2 wt% Al_2O_3 (AKP30 grade, Sumitomo Chemical Co., Osaka, Japan)) and 6 wt% Y_2O_3 (fine grade; Herman C. Starck, Berlin, Germany) as sintering additives were ball milled in methyl-isobutyl ketone for 24 hours. After 2, 5, and 10 wt% β-Si_3N_4 whisker (SN-WB, 0.1–1.5 μm in diameter, 10–15 μm in length and aspect ratio of 20–100, UBE Industries, Yamaguchi, Japan) were added into the above slurry, the mixtures were ball milled once more for 4 hours. The composite slurry with binder (21 wt% of polyvinyl butyral; Aldrich Chemical Co., Milwaukee, U. S. A.), dispersant (3 wt% of Hypermer KD-1; ICI Chemical Co., Barcelona, Spain), and plasticizer (14 wt% of dibutyl phthalate; Aldrich Chemical Co.) was ball milled for 1 hour. The slurry was in vacuum for one hour to get deairing and was poured in the slurry dam of the modified tape casting machine. Modification of the tape casting was performed by placing two rows of pins which were 0.7 mm apart from each other, in each row at the exit of the slurry dam and dividing the flow of slip into 215 narrow ones each of which have velocity distribution curve $(215)^2$ times as drying, the tape was cut into 36×36 mm^2 size sheets which were about 120 μm in thickness. The sheets were stacked in the unidirectional alignment of β-Si_3N_4 whisker. After lamination at 363 K, under 50 MPa for one hour, the stacked body was about 8 mm thick. The specimens were cold isostatically pressed under 250 MPa. After then binder was burnt out at 823 K in air for a week. The debinded specimens were fired at a constant heating rate of 773 K/h and maintained at different temperatures depending on the amount of β-silicon nitride whiskers (as shown in Table I) for 4 hours in 3 MPa nitrogen gas.

2.2. Evaluation methods

After sintering, bulk density of gas pressure sintered specimens was measured by the water immersion method. Microvickers hardness tests were carried out under a load of 9.8 N, and Vickers indentation crack lengths were generated by using a load of 196 N. Indentation cracks were produced in such a way that the two cracks were parallel to and normal to the tape casting direction, respectively. The mechanical properties are displayed in Table I.

The microstructure of the Gas Pressure Sintered materials with undirectrionally oriented and elongated grains was examined by scanning electron microscopy (SEM) of polished and plasma etched surfaces using a commercial plasma etching apparatus (RF Plasma Barrel Etcher PT 7150, Bio Rad Laboratoric GmbH, Munich, FGR). The etchant gas was mixture of $CF_4 + 5$ vol% O_2 adjusted to a total pressure of 0.3 mbar. Etching was conducted at 100 W for up to 10 minutes. TEM foil preparation was performed by standard technique involving grinding, dimpling, Ar-ion milling to perforation, and subsequent coating with a thin carbon film to minimize electrical discharging in the microscope. Microstructural characterization of specimen was performed by conventional transmission electron microscopy (Model H-8100T, Hitachi, Japan). Identification of crystalline secondary phases formed upon densification was performed by both X-ray diffraction (XRD). XRD was performed with Cu K_α radiation under 25 kV and 35 mA. The scan speed was 4°/min and 2θ varied from 10° to 80°. XRD patterns were obtained from the tape casting plane.

2.3. Thermal conductivity measurement

A heater was attached on one end of the silicon nitride with Ag paste and the other end was thermally grounded to the Cu-block of the sample holder. Strain gauge of resistance 350 ohms, 2×4 mm^2, was used for the heater. The schematic diagram for thermal conductivity measurement is presented in Fig. 1. The resistance of the heater was monitored throughout the range to measure the Joule heating power input to the sample. Three calibrated T-type thermocouples were

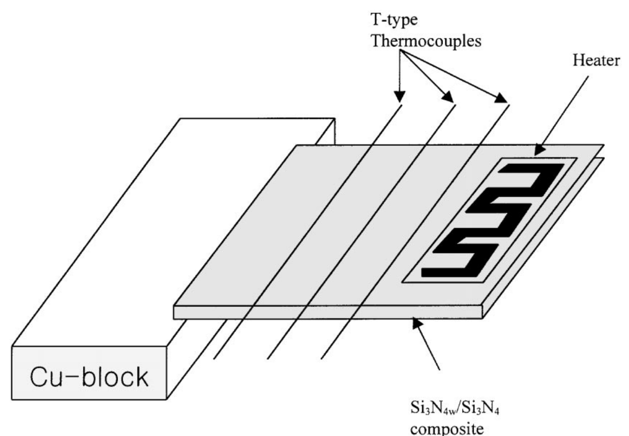

Figure 1 The schematic diagram for measurement of thermal conductivity. One end of the sample is thermally grounded to the Cu-block. The other end was attached by an electric resistance heater (strain gauge with resistance 350 Ohms). Three thermocouples were attached 2–3 mm apart each to measure thermal gradient. Heat loss through the wires is less than 1% of total input power.

TABLE I Test samples and their mechanical properties

Sample	Whisker content (wt%)	Sintering temperature (K)	Relative density (%)	Hv (Kg/mm^2)	K_{IC} (Mpam$^{1/2}$) //	K_{IC} (Mpam$^{1/2}$) ⊥
2W	2	2123	97.5	1406	4.8	6.5
5W	5	2148	98.5	1340	4.5	7.5
10W	10	2273	97.1	1280	4.2	10.1

// and ⊥ : in parallel and perpendicular directions with respect to the tape casting direction.

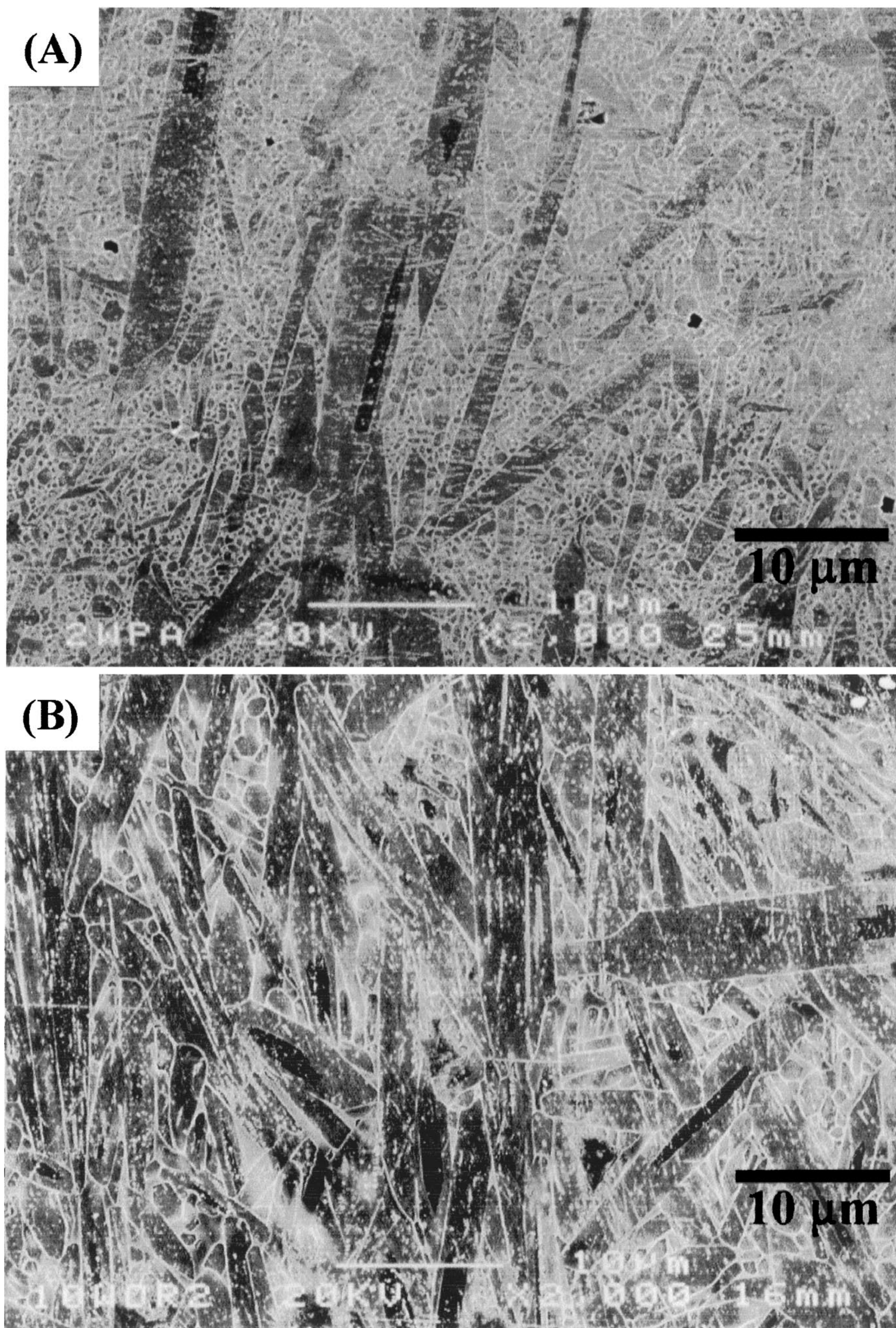

Figure 2 SEM micrographs of the etched surfaces in the β - Si_3N_4 whisker reinforced Si_3N_4 composites; (A) 2 wt% β - Si_3N_4 whisker and (B) 10 wt% β - Si_3N_4 whisker addition.

attached on the sample, 2–3 mm apart each to measure the thermal gradient with a temperature resolution $\leq$10 mK. The distance between the thermocouples was measured by a cathetometer within 10 μm. In Fig. 1, the junction size of the thermocouple is drawn larger than the real size. The thermocouples were attached by small amount of Ag-epoxy. The diameter of the junction including Ag-epoxy is less than 80 μm. The diameter of Cu-wire from the heater and the thermocouple wires 0.025 mm. Heat losses through the wires less than 1% of the total power input. Thermal conductivity was measured in vacuum to avoid the heat loss by convection. Thermal conductivity of specimen was measured only from 293 K to 373 K.

3. Results and discussion

3.1. Microstructure

Fig. 2 illustrates the etched surfaces of Si_3N_4 composites added with different amount of β-Si_3N_4 whiskers. The microstructure around the large elongated grains shows small grains surrounded with the glassy grain boundary phases. The elongated grains were aligned unidirectionally, which were parallel to the tape casting

direction. The higher content of β-Si_3N_4 whiskers seemed to be relatively easy for unidirectional alignment. Growth of the elongated β - Si_3N_4 grain was suppressed in the parallel orientation to the tape casting direction because the long axes of the elongated β - Si_3N_4 grain including with whisker were joined together. This phenomena is illustrated in Fig. 2b. The elongated grains of 10 wt% β-Si_3N_4 whisker added into Si_3N_4 composite are relatively more aligned to the same direction. The processing pores were also observed. Porosity may increase significantly when the β-Si_3N_4 whiskers in the composites are added over 10 wt%.

In this study, the sintering temperatures were changed to govern the porosity as the content of β-Si_3N_4 whiskers in the composites increased from 2 wt% to 10 wt%, which is displayed in Table I. Relative densities of both samples are almost same value of 97%, which does not indicate the full densification. Hereafter, the sintering temperature and sintering holding time should be combined to improve the density and sinterbility if the composite of higher contents of β-Si_3N_4 whisker be fabricated.

The preferred orientation of the large elongated grains were analyzed by x-ray diffraction. Matrix grains of the composite without whiskers may be randomly oriented and that some of matrix grains disappeared during sintering as whiskers were added. Fig. 3 shows XRD patterns of the samples after sintering. Patterns from the tape casting plane show strong peaks for the (210), (200), (110), (320), (310) and (100) planes. As shown in Fig. 3, the main planes of grain growth of the whisker grains are (210) and (200), which are the same major planes of β-Si_3N_4 phase. Intensities for the (101) and (202) peaks decreased as the whisker content increased up to 10 wt%, while (210), (200), and (110) peaks became stronger. The XRD spectrum of the 10 wt% whisker composite shows double peaks at the angle of 33° (2θ). These two peaks may be $Y_{20}N_4Si_{12}O_{18}$ as the grain boundary phase after sintering at 2273 K. Abe [12] investigated the influence of additive composition on the grain boundary phase of Y_2O_3 and Al_2O_3 doped Si_3N_4 after quenching the sintered body. It was suggested that the relative amount

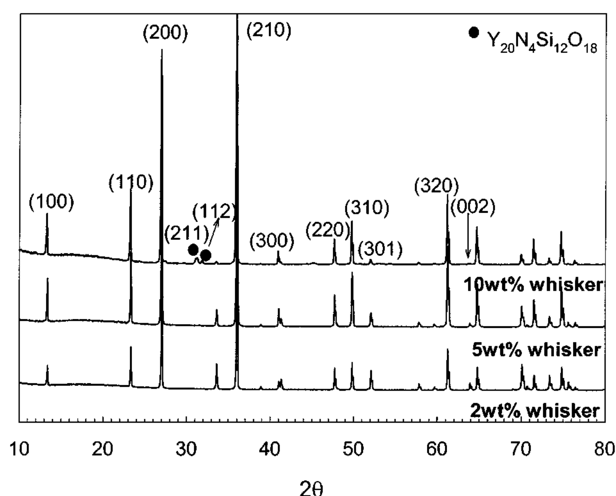

Figure 3 XRD patterns of the Si_3N_{4w}/Si_3N_4 composites.

of grain boundary phases detected in quenched samples and the formation of Si_2N_2O restricted densification below 1873 K. The shrinkage of the sintered body above 2023 K was closely corresponding to the formation of $Y_2Si_2O_7$.

The microstructures were observed by scanning electron microscopy as well as transmission electron microscopy to understand the interfaces among the large elongated grains, relatively small grains, and grain boundary phases.

Fig. 4 indicates SEM and TEM morphologies of the 2 wt% of whisker content in the composite. A dislocation line imperfection inside the large elongated grains which were grown by Si_3N_4 whisker as a seed, is observed.

3.2. Thermal conductivity

Fig. 5 shows the variation of thermal conductivity of different whisker content into Si_3N_4 composites from 298 K to 373 K in the parallel direction to the tape casting plane. The thermal conductivity decreases with increasing temperature. The temperature dependence of thermal conductivity of the four samples (HP-, HIP-, RS-, CVD-Si_3N_4) was investigated in the previous works [1–6]. It was reported that the thermal conductivity of CVD- Si_3N_4 decreased with increasing temperature from 58.8 Wm^{-1} K^{-1} at 293 K to 19.6 Wm^{-1} K^{-1} at 1573 K [1]. The crystalline CVD- Si_3N_4 exhibited the negative temperature dependence of thermal conductivity, while the amorphous CVD- Si_3N_4 showed a positive temperature dependence of thermal conductivity. However, the amorphous CVD- Si_3N_4 exhibited the a positive temperature dependence of thermal conductivity.

In Fig. 2b, it was shown that that the higher content of β-Si_3N_4 whiskers illustrated relatively unidirectional orientation of the elongated grains growing from the whisker. The higher content of whisker provides the higher interconnection of the elongated grains. The interconnection of the elongated β - Si_3N_4 grain enhanced the thermal conductivity in the parallel orientation to the tape casting direction because the phonon can be transferred into the long axes of the elongated β - Si_3N_4 grain even though it includes dislocation at the boundary of the core/shell structure.

Fig. 6 shows the comparison of thermal conductivities of 10 wt% whisker content sample between in the parallel direction and in the perpendicular direction. For HP- Si_3N_4, the observed anisotropy of thermal conductivity was thought to be related to the formation of elongated grains [8]. Moreover, a strong orientation effect on thermal diffusivity/conductivity can be obtained. The reason for this was that the elongated β-grains exhibited a preferred orientation in such a way that their direction of elongation, which coincided with the crystallographic c-axis of the hexagonal β-phase, was oriented perpendicular to the hot-pressing. This preferred orientation has been shown to result also in a pronounced anisotropy in strength and fracture toughness. Moreover, thermal conductivity of dense Si_3N_4 is influenced by other microstructural parameters such as the amount of glassy phase and solid solution

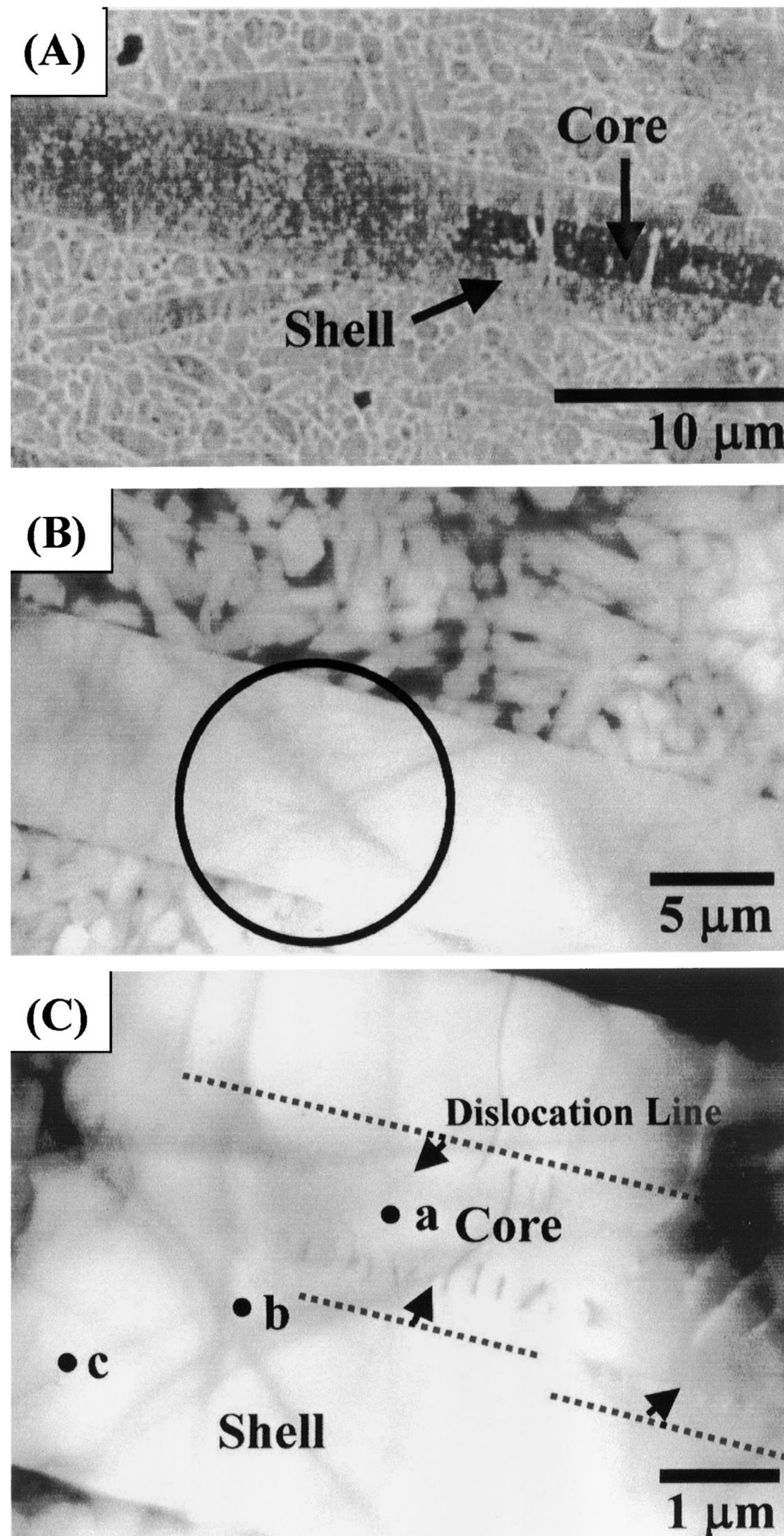

Figure 4 SEM (A) and TEM (B) micrographs (and its high magnification (C)) of core/shell structure for the 2 wt% β - Si_3N_4 whisker reinforced Si_3N_4 composite.

effects. The use of sintering aids changes the physical properties of hot-pressed Si_3N_4 markedly. The thermal diffusivity/conductivity values of silicon nitride without additives were lower than those of the densely chemical vapor deposited silicon nitride as reported by Hirai *et al.* [1]. Considering that the chemical vapor deposited silicon nitride was perfectly dense, high pure, and no grain boundary phase, the lower values of the gas pressure sintered specimen apparently were due to the presence of grain boundary phases and a small amount of porosity. The thermal conductivity values of these sintered bodies became smaller in the following order: $Si_3N_4 > Si_3N_4 + MgO > Si_3N_4 + Y_2O_3 > Si_3N_4 + Al_2O_3$. It was thought that the lower thermal conductivity of Si_3N_4 bodies with additives were due to the presence of a glassy phase at the grain boundaries, because the thermal conductivity of the glassy phase is lower than that of the crystalline Si_3N_4 phase [3].

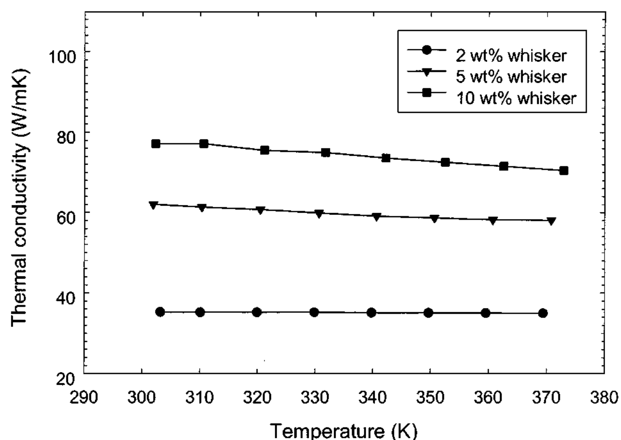

Figure 5 Temperature dependence of the thermal conductivity in the parallel direction of Si_3N_{4w}/Si_3N_4 composites.

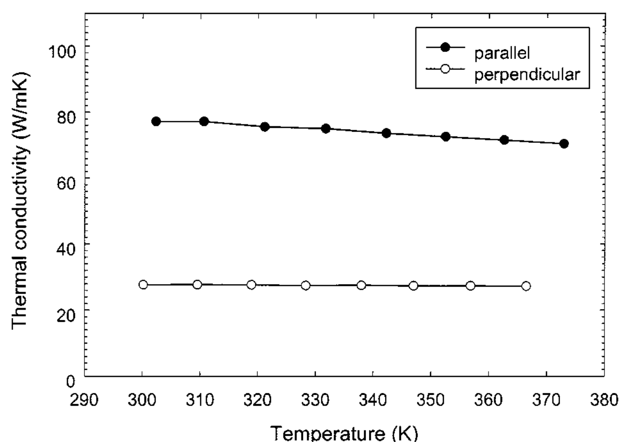

Figure 6 Comparison of thermal conductivity between in the perpendicular direction and in the parallel direction for 10 wt% β - Si_3N_4 whisker reinforced Si_3N_4 composite.

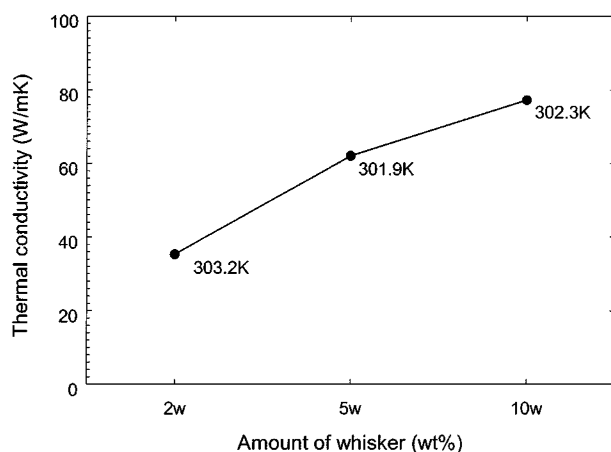

Figure 7 Variation of thermal conductivity as a function of the amount of Silicon nitride whisker.

Addition of Al_2O_3 degrades thermal conductivity. Kuriyama *et al.* [2] reported that the lower thermal conductivities of hot pressed Si_3N_4 - Al_2O_3 were explained by the presence of an "X phase" at the grain boundary together with the formation of the solid solution (a compounding having a mullite-like structure; $Si_4Al_4O_{11}N_2$).

Fig. 7 shows the effect of the whisker content in silicon nitride on the thermal conductivity at room temperature. The thermal conductivity increases linearly with increasing the amount of the large elongated grains. Watari *et al.* [13] reported that thermal conductivity of silicon nitride at room temperature is not controlled by the grain size, but rather the internal defects of the grains, such as dislocations and point defects. The reason was that the calculated phonon mean free path length (about 20 nm) was an order of magnitude smaller than the smallest grain sizes in the sintered silicon nitride samples. If the phonons are scattered significantly by the presence of a grain boundary at room temperature, the phonon mean free path must equal the magnitude of the grain size. Therefore, the thermal conductivity in the perpendicular direction should be independent on the width as well as the amount of the elongated grains in this composites. The elongated grain length of β-silicon nitride influences the thermal conductivity of silicon nitride. Hirosaki *et al.* [14] showed the influence of grain growth on thermal conductivity of β-silicon nitride with increasing sintering temperature up to 2473 K. They showed that higher thermal conductivities were established by growth of Si_3N_4 grains and decrease in the amount of two-grain junction. In most cases, oxidation products cause a decrease in thermal diffusivity/conductivity which was dependent on the type and penetration depth of the oxidation products. Oxygen produces defects inside α-Si_3N_4, but no defects in β- Si_3N_4. Fig. 4 showed the dislocations inside the elongated grains in the area of core/shell. These dislocation provide the phonon-imperfection scattering and degrade the thermal conductivity. These dislocations are attributed to solid solution with Al_2O_3 in the elongated grains, and this solid solution of Al_2O_3 into the Si_3N_4 in the shell area was identified by EDX analaysis with TEM, as mentioned in previous work [15]. Slack and his coworkers hypothesized that the low thermal conductivity of Si_3N_4 [16] and AlN [17] without any additive has been attributed to impurities. The effect of impurities of thermal conductivity of AlN, in particularly oxygen, has been investigated experimentally and explained on the basis of the thermodynamics [18].

4. Conclusions

From the experimental results, the following conclusions are made.

1) Thermal conductivity is dependent upon the orientation of whisker alignments. Thermal conductivity in the direction to the tape casting direction is 1.5 times that in the perpendicular direction. Interconnection of the elongated β -Si_3N_4 grains enhances thermal conductivity to the tape casting direction because the long axes of the elongated β - Si_3N_4 grain including with whisker were joined together.

2) Thermal conductivity of the unidirectionally aligned Si_3N_4 whisker reinforced Si_3N_4 composites increased with increasing the amount of Si_3N_4 whisker in the composites. Interconnection of the elongated β -Si_3N_4 grains due to the grain growth into the long axes of the elongated β - Si_3N_4 grain including with whisker were enhanced with increasing the amount of β - Si_3N_4 whisker in the composites.

3) The large elongated grains contains the core/shell structure, which exhibited the dislocations. These defects degrade the thermal conductivity due to the phonon scattering.

Acknowledgements
This work was supported by the Korea Research Foundation (grant no. 1997-011-E 00028). Also the authors acknowledge Dr. Michiyuki Suzuki and Dr. Yamada of the UBE industries for providing silicon nitride whiskers.

References
1. T. HIRAI, S. HAYASHI and K. NIIHARA, *Am. Ceram. Soc. Bull.* **57** (1978) 1126.
2. M. KURIYAMA, Y. INOMAT, T. KIJIMA and HASEGAWA, *ibid.* **57** (1978) 1119.
3. K. TSUKUMA, M. SHIMADA and M. KOIZUMI, *ibid.* **60** (1981) 910.
4. K. HAYASHI, S. TSUJIMOTO, T. NISHIKAWA and Y. IMAMURA, *J. Ceram. Soc. Jpn.* **94** (1986) 595.
5. K. WATARI, Y. SEKI and K. ISHIZAKI, *ibid.* **97** (1989) 56.
6. *Idem.*, *ibid.* **97** (1989) 174.
7. G. ZIEGLER and D. P. H. HASSRELMAN, *J. Mater. Sci.* **16** (1981) 495.
8. G. ZIEGLER, in “Progress in Nitrogen Ceramics,” edited by F. L. RILEY (Martinus Nijhoff Publishers, Boston, 1983) p. 565.
9. J. S. HAGGERTY and A. LIGHTFOOT, *Ceram. Eng. Sci. Proc.* **16** (1995) 475.
10. N. HIROSAKI, Y. OKAMOTO, M. ANDO, F. MUNAKATA and Y. AKIMUNE, *J. Am. Ceram. Soc.* **79** (1996) 2878.
11. K. HIRAO, W. WATARI, M. E. BRITO, M. TORIYAMA and S. KANZAKI, *ibid.* **79** (1996) 2485.
12. O. ABE, in the 1st International Symposium On the Science of Engineering Ceramics, 1991, edited by K. NIIHARA, p. 89.
13. K. WATARI, K. HIRAO, M. TORIYAMA and K. ISHIZAKI, *ibid.* **82** (1999) 777.
14. N. HIROSAKI and A. OKADA, *ibid.* **72** (1989) 2359.
15. S. W. LEE, D. S. PARK, Y. H. CHOA and K. NIIHARA, *J. European Ceram. Soc.* in contribution.
16. G. A. SLACK and I. C. HUSEBY, *J. Appl. Phys.* **53** (1982) 6817.
17. G. A. SLACK, R. A. TANZILLI, R. O. POHL and J. W. VANDERSANDE, *J. Phys. Chem. Solids* **48** (1987) 641.
18. A. V. VIRKAR, T. B. JACKSON and R. A. CUTLER, *J. Am. Ceram. Soc.* **72** (1989) 2031.

Received 19 January
and accepted 16 February 2000